



**U.S. Department of Energy
2020 Collegiate Wind Competition
Technical Design Report**

University of Wisconsin-Madison

Electrical Sub-team: Davis Wade (<i>EE Team Lead</i>) Michael Craney Justin Casleton Truman Kent Fotios Emery	Mechanical Sub-team: Brad Tschoeke (<i>ME Team Lead</i>) Louis Liu Scott Underwood Tyler Orcutt Joseph Fernandez	Principal Investigator Scott Williams Faculty/Staff Advisors: Randy Jackson Kyle Hanson Contact spwilliams@wisc.edu
---	--	--

Table of Contents

Executive Summary	3
Introduction	4
Mechanical	4
Mechanical Design Objectives	4
Blades	4
Design Parameters and Airfoil Selection	5
Airfoil Analysis	6
Blade Design in QBlade	7
Blade Simulation and Manufacturing	8
Pitch Control	9
Mechanical Design Parameters and Pitch Control System	10
Feedback Control System	11
Nacelle and Yaw Control	12
Electromechanical	13
Electromechanical Design Objectives	13
Mechanical Design	13
Design Constraints	13
Stationary Components	13
Rotating Assembly	13
Electrical Design	14
Design Constraints	14
Magnets	14
Coils	14
Modular Design	16
Output of generator board	16
Safety Module	17
Testing and Results	18
Testing of Emergency Braking	18
Conclusion	19
References	20

Executive Summary

WiscWind is an interdisciplinary engineering student organization competing in the U.S. Department of Energy 2020 Collegiate Wind Competition (CWC), giving students real-world experience in the growing renewable energy industry. The mechanical and electrical sub-teams are tasked with designing and fabricating a wind-driven power system that maximizes power generation and can accomplish specific tasks detailed in the competition rules.

The mechanical sub-team completed research on last year's design to improve results from the 2019 competition. The major tasks this year have included, but are not limited to, beginning rework on the blade design, implementation of an active pitch control system, and further research for the pitch and yaw controls. All of these factors have been worked on to improve the mechanical efficiency of the turbine. This will allow a greater speed of the shaft for a given wind speed, which creates a greater power output. With a greater power output, the team would have scored higher marks in the many categories of the wind tunnel test. The fall semester was dedicated to further research, preliminary testing and implementation of the new blade designs, with plans of developing and implementing the pitch and yaw controls in the spring semester.

The electrical sub-team focused on converting the mechanical energy captured by the wind into electrical energy. This was accomplished with a custom made three-phase axial flux generator which was designed by members of the electrical and mechanical teams and fabricated by members of the mechanical team. Power electronic circuits control high efficiency three-phase AC to DC conversion, electrical noise suppression, emergency load disconnection, and emergency braking using an Arduino microcontroller and a combination of hand built and off the shelf circuitry. The fall semester was dedicated to the creation of new stators for the generator. The team's main focus was to determine the correct balance between coil turns and wire thickness as well as improving the direction of magnetic field lines and to improve the flux linkage between the two opposing plates of magnets in the rotors. The spring semester was initially dedicated to the creation of control and power circuitry, however COVID-19 quickly put a halt to any in-person meetings or on-campus wind tunnel usage. The only electrical system prototype that was created was the electronic braking system.

Our mechanical and electrical designs have been an iterative process. All parts were purchased, machined, and assembled by members of the team. Most components have been tested individually both in the wind tunnel and on the dynamometer. Despite being unable to complete the wind turbine, we were feeling confident of its abilities and the little amount of testing we were able to complete delivered very promising results. We believe our designs to be sound and able to be very competitive against others' in the competition, especially if we were able to test for unforeseen obstacles on physical prototypes.

Introduction

WiscWind's development and design for the prototype turbine focused on optimizing performance at cut-in and low wind speeds and maximizing the turbine power output over all wind speeds. This is achieved through several power saving features such as improved blades optimized for low speed efficiency, and a generator design which eliminates cogging torque. Converting the mechanical energy captured by the wind into electrical energy is accomplished with a custom made three-phase axial flux generator. Power electronics circuits control AC to DC conversion, power regulation, and emergency braking.

Mechanical

Mechanical Design Objectives

WiscWind's top priorities in its design were achieving both a low cut-in speed and stable power curve with a large rated region. In order to meet these criteria, the blades and control systems have been designed with the balance of these requirements in mind. The blade geometry controls the cut-in speed of the wind turbine and the control systems ensure that the power curve is stable and predictable across a wide range of wind speeds. While there are many other subsystems of the wind turbine including the nacelle and tower subassemblies, they do not have as much of an impact on the desired performance abilities of the wind turbine as the blades and control systems. A CAD model and assembly of our prototype wind turbine can be seen in Figure 1 below.

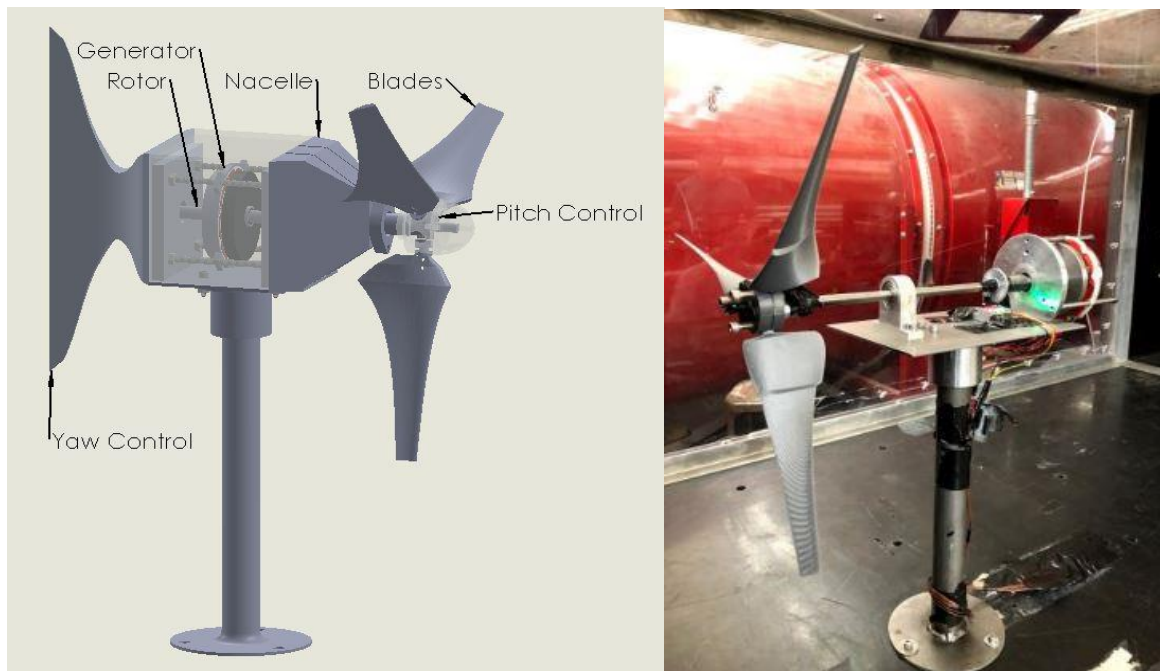


Figure 1. (L) Turbine prototype CAD model; (R) Prototype turbine assembly in wind tunnel test

Blades

Before beginning the blade design process, it is important to determine the goals, or desired blade characteristics. These can be inferred from investigating which of the competition tasks can be impacted by the blades. Figure 2 plots the power output vs. wind speed required by the competition.

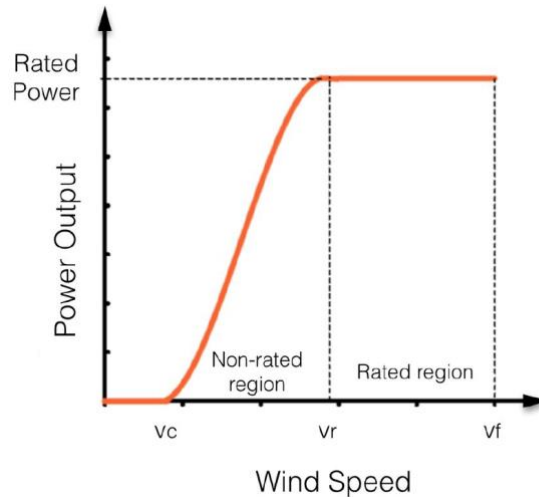


Figure 2. Desired power curve for competition testing scenario [1].

The cut-in wind speed, V_c , is the speed at which the turbine starts generating power. The cut-in wind speed is influenced more by the root of the blade than the tip, meaning that proper design of the root can minimize the cut-in wind speed. The non-rated region, from 5-11 m/s, is where the turbine will produce maximum power output. Lastly, in the rated region of 11-18 m/s, the power output and rotational speed of the turbine must remain constant. Proper design of the turbine blades can help the team excel in these competition tasks.

Design Parameters and Airfoil Selection

The first step in designing a turbine rotor that harnesses maximum energy from the wind is developing an optimal airfoil design. Research on previous teams' designs revealed a few airfoils that experienced success in past competitions: the Wortmann FX 63-137 and the SG 6043 airfoils. The SG 6043 airfoil was used in conjunction with the Wortmann FX 63-137 in a blade that contained multiple airfoil cross sections. While this can help improve cut-in wind speed performance, WiscWind's active pitch control system will have a greater effect on lowering cut-in wind speed, leading us to move forward with a single airfoil blade. The airfoil selected was the Wortmann FX 63-137, which was selected due to its slim profile which will minimize drag for a model-scale turbine.

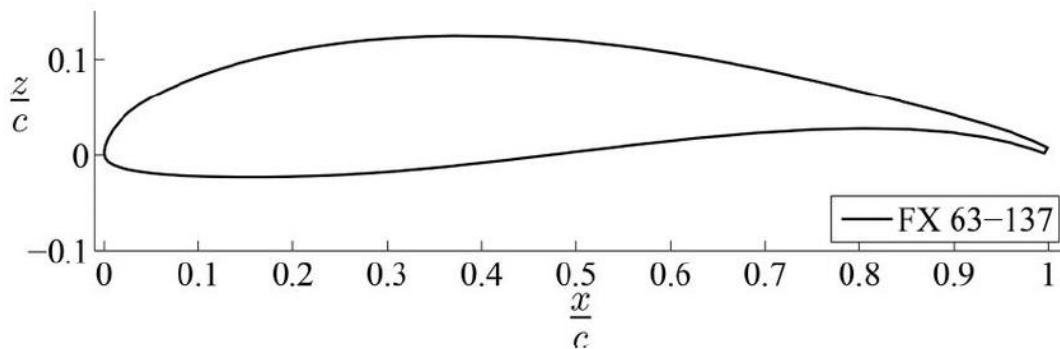


Figure 3. Wortmann FX 63-137 airfoil used in blade design

In addition to determining which airfoil cross sections to pursue, extensive research was done to determine the optimal number of blades for turbine performance. Even blade numbers tend to cause cyclical loading on the drivetrain. While this isn't as much of a concern at the scale we are working at, we decided to move forward with three and five blade designs. Several aspects of five-blade turbines may be beneficial to our competition performance, including a lower cut-in wind speed and higher power production at low wind speeds (<11 m/s). However, there are also aspects that could hinder performance, including higher drag due to increased surface area on the blades and the risk of moving past the Betz Limit. The Betz Limit states that a maximum of 59% of the wind's kinetic energy can be extracted by a turbine [2]. Blocking too much

of the airflow will result in the buildup of stagnant air behind the rotor, preventing more air from coming through the turbine. In addition, a five-blade design would be significantly more difficult to develop a pitch control system for, as the hub area to work with is limited. Because of the strong potential advantages of using a five-blade design, the team decided to pursue both a three-blade and five-blade design for testing in the wind tunnel to determine which performs better.

Airfoil Analysis

When trying to assess the performance of an airfoil and design a blade to maximize power output, there are a number of airfoil characteristics that must be investigated. These characteristics include a large lift coefficient and a high lift to drag ratio, in addition to the angle attack at which the maximum lift to drag ratio occurs. These important parameters depend on the Reynolds' number, which is the ratio of inertial forces to viscous forces in a flow, given below in Equation 1:

$$Re = \frac{\rho V L}{\mu} \quad (1)$$

where L is the characteristic length of the flow, ρ is air density, μ is the viscosity of the air, and V is the velocity of the flow. For wind turbine blades, the characteristic length is defined as the chord length, which is the distance from the leading edge of the airfoil to the trailing edge, shown in Figure 4 below.

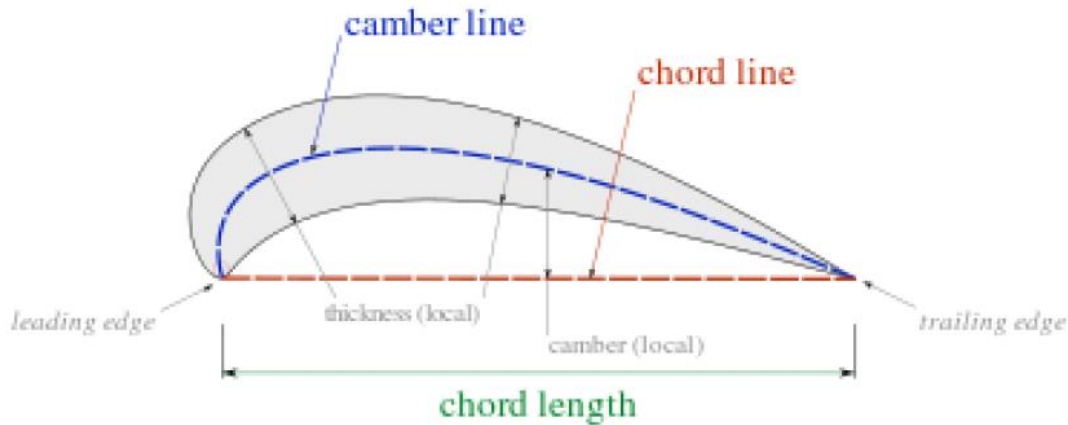


Figure 4. Diagram of airfoil, showing the chord length in relation to leading and trailing edge [3].

Knowing the air density and viscosity at the testing site in Denver and the range of testing wind velocities and chord lengths, a range of operational Reynolds' numbers can be found for the competition. It is important to note that the competition site in Denver has an air density of 0.96 kg/m^3 , while our testing site in Madison has an air density of 1.2 kg/m^3 . The densities and corresponding Reynolds' numbers differ by $\sim 20\%$, meaning that the flow characteristics are significantly different [4]. At the competition in Denver, the turbine is expected to operate in Reynolds' numbers ranging from $\sim 10,000$ - $40,000$, placing it in the laminar flow region. In order to gain important information about the characteristics of the chosen airfoil, XFOIL, an open source airfoil analysis software, was utilized. XFOIL calculates the pressure distribution of flow over an airfoil and uses the pressure distribution data to determine lift and drag characteristics. The Reynolds number is an important input in XFOIL analysis, as airfoils have unique performance curves at every Reynolds number. Shown below is the ratio of lift coefficient to drag coefficient vs. the angle of attack (C_L / C_D vs. α) for the Wortmann FX 63-137 airfoil, the airfoil selected for competition.

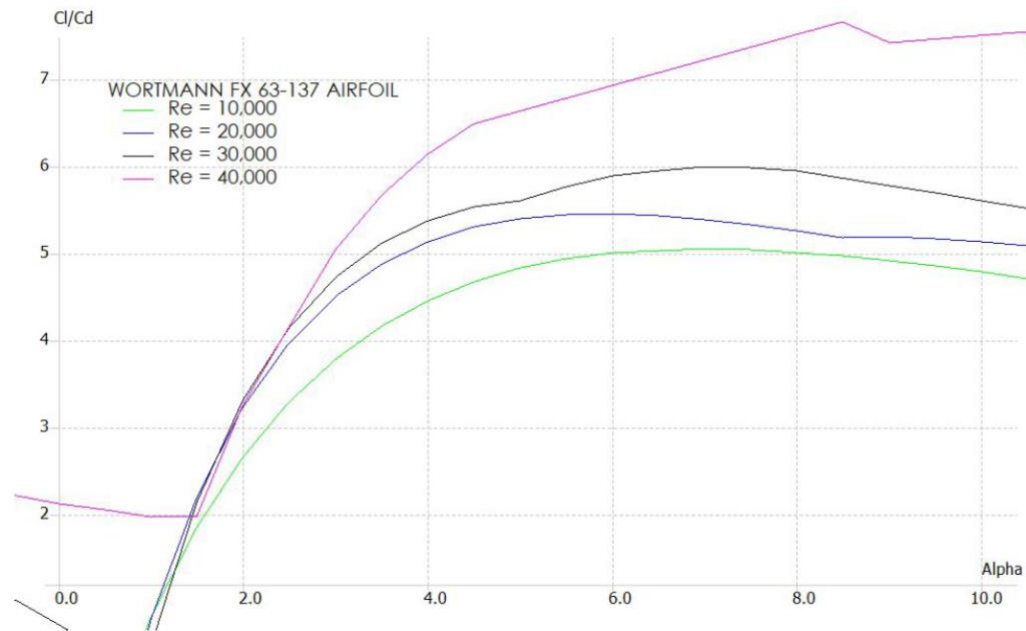


Figure 5. C_L / C_D vs. alpha curve for Wortmann FX 63-137 airfoil.

The various curves correspond to different Reynolds numbers, showing that the airfoil has different characteristics depending on which Reynolds number it is operated at. One important takeaway from the above figure is the angle of attack at maximum C_L / C_D . This angle of attack will maximize the lift force, which helps propel the blade and generate power, while minimizing the drag force, which acts opposite the motion of the blade. The angle of attack at optimal C_L / C_D ratio is between 5 and 9 degrees, depending on the Reynolds number.

Blade Design in QBlade

QBlade is an open-source wind turbine design and analysis software, perfect for developing and simulating blade designs for the competition turbine. After importing the Xfoil analyses and extrapolating them to three dimensions, the blade design process begins. To accommodate the pitch control system, the radius of the hub must be 3.2 cm. To maximize the competition space requirements, the blades were made to be 19.3 cm long, maximizing the 22.5 cm space allowed. A total of 40 panels along the span (length) of the blade were chosen to discretize the design, in order to smoothen the contours of the blade.

Optimization in QBlade comes in two forms: chord length optimization and twist angle optimization. The twist angle is optimized according to the optimal angle of attack for the airfoil profile used, accounting for the velocity vector changing direction along the span of the blade due to the rotational component. The chord length has two optimization options, the Schmitz method and the Betz method. The main difference between these two methods is that the Betz method only accounts for axial downstream losses, while the Schmitz method accounts for axial losses as well as downstream swirl losses due to the rotation of the turbine wake [5]. Because the Schmitz method accounts more accurately for losses, it will be used for all turbine designs.

An important principle governing wind turbine performance is the tip speed ratio (TSR) of the blades. The TSR is defined as the ratio of the velocity of the tip of the blades to the wind velocity. This formula is shown by Equation 2 below.

$$\lambda = \frac{\omega R}{V} \quad (2)$$

The optimal TSR for three-bladed commercial wind turbines is typically seven, but through trial and error of various turbine blade designs it was determined that a TSR of 5.5 is more practical for a turbine of this scale. This corresponds to an angular velocity of approximately 2500 rpm at a wind velocity of 11 m/s, which helps limit the risk of fatigue failure on the blades. After performing the optimizations discussed and smoothing the contours of the blade, the following design was selected for final testing.

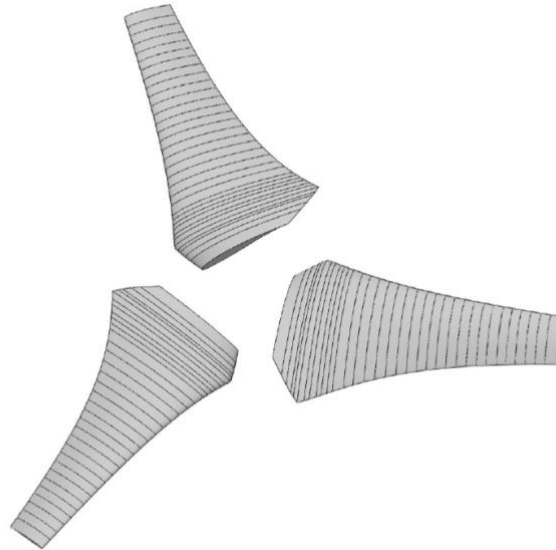


Figure 6. Final blade design developed using QBlade optimization.

Blade Simulation and Manufacturing

On top of the optimization and design features, QBlade also contains powerful blade performance simulation features. This allows the user to simulate blade performance at a variety of Reynolds numbers, wind velocities, angles of attack, and rotational speeds. Shown below in Figure 7 is the power output vs. TSR curve for wind speeds ranging from 5-11 m/s.

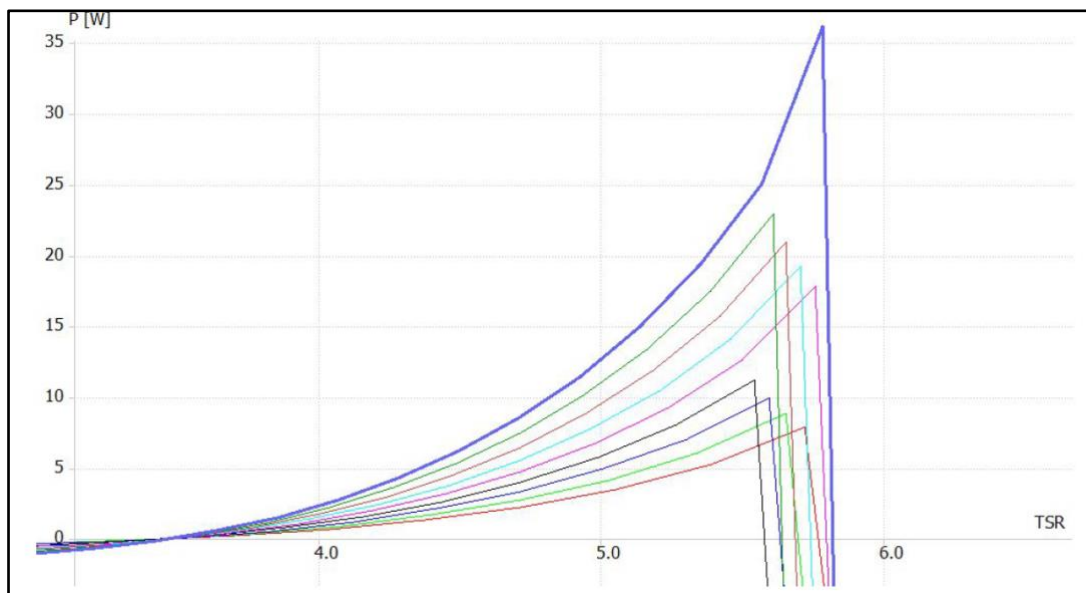


Figure 7. Power curve for final blade design. Different colored curves correspond to different wind speeds.

The blue curve corresponds to the highest wind speed tested (11 m/s) and the red curve corresponds to the lowest wind speed (7 m/s), with increments of 0.5 m/s in between. The turbine is predicted to produce approximately 35 Watts of power at 11 m/s, which is the highest wind speed tested in the power curve portion of the competition. This power output is consistent with the performance of previous competition teams' designs and proves the legitimacy of the design.

After development of the blade design, it is important to determine a method of manufacturing. The blades were manufactured using additive manufacturing on a 3D printer with Polylactic Acid (PLA)

filament. The blades were printed vertically with water-soluble PVA support structures. Vertical printing improves surface finish as opposed to horizontal printing, as layer thickness was too large to produce smooth contours. A smooth surface finish is critical for our blade performance, as any roughness could disrupt the flow and reduce the lift on the blade. Another option to improve surface quality is to coat the blade with a type of epoxy which will fill in the roughness and result in a smooth blade.

It is important to consider the structural integrity of the blades as well. QBlade is also able to simulate the loads at certain wind speeds and run a Finite Element Analysis (FEA) of the blades. Shown below is the result of the FEA at a wind speed of 26 m/s, the highest wind speed tested in the competition

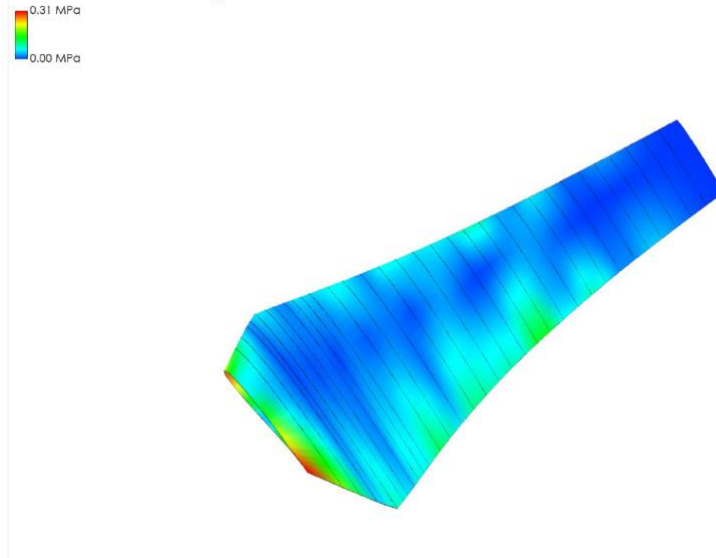


Figure 8. FEA for final blade design, assuming a wind velocity of 26 m/s.

As shown in Figure 8 above, the maximum stress on the blade is 0.31 MPa at the corners of the root of the blade. Considering PLA has a minimum yield strength of 2 MPa, the maximum stress of 0.31 MPa provides a factor of safety of 6.25. This provides ample assurance that the blades will hold up to the durability tests of the competition.

Pitch Control

Pitch control is the process of altering the angle of attack of our blades to adjust the amount of power that the turbine system draws from the kinetic energy of the wind. Typically, on commercial wind turbines, there are two types of power control strategies: active pitch control, and passive control. Active pitch control relies on a feedback loop to control motors or hydraulics to shift the power output to the desired amount, whereas passive power control doesn't require a feedback loop. Some larger turbines use fixed pitch blades that are designed to stall in strong wind conditions, effectively controlling their maximum rotational speed. WiscWind's 2019 design attempted to employ a passive pitch control system, where the angle of the blades was controlled by the centripetal force acting on the turbine, much like a flyball governor. The advantage of using a passive pitch control design is that no electricity needs to be drawn from the generator to power the system. However, a large disadvantage is the increased mechanical complexity and difficulty in tuning, in addition to the added moment of inertia.

Mechanical Design Parameters and Pitch Control System

The main objective of WiscWind's pitch control system was to regulate the turbine rotational speed and power output over a variety of wind velocities. Two goals are to optimize the cut-in wind speed and power output at low wind velocities, and to maintain the rated power output at wind velocities over 11 m/s. Working under a strict timeline, the ease of design and manufacturability of the system were heavily considered. Because of the desire to optimize our power curve at low wind velocities, a

stall-controlled system would not be feasible as it only regulates the maximum power output of the turbine.

The choices then were to either alter last year's passive pitch control design or design an active pitch control system from scratch. Last year, the passive pitch control system had serious issues with the responsiveness to changes in wind velocity due to the friction between the components. The percent change in centripetal force was not large enough to reliably change the pitch of the blades. The team believed that employing this system would require extra time to redesign, manufacture, and tune due to its complexity, and the system would still lack the active feedback loop that can prove invaluable in competition. In comparison, the expected voltage draw of an active pitch control system consisting of an Arduino and a servo motor was about 8 V, compared to an expected voltage output of 36 V, the active pitch control system was determined to be more suitable for this year's competition turbine.

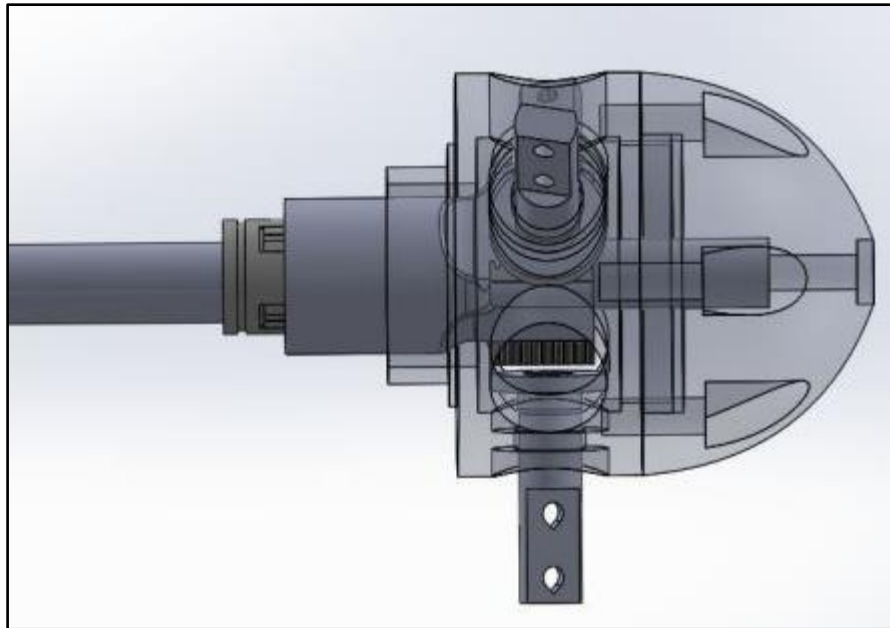


Figure 9: Pitch control mechanism inside rotor hub

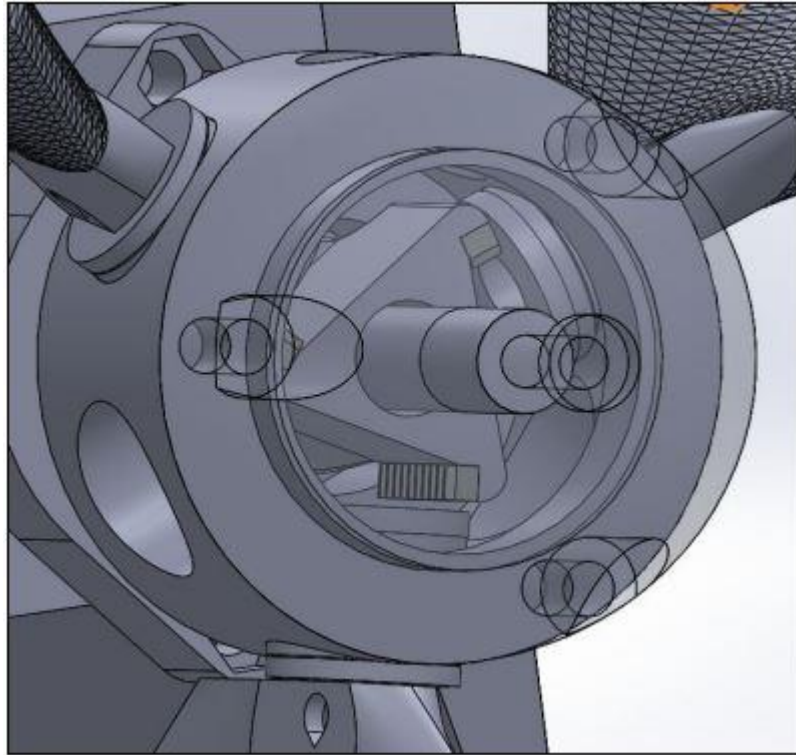


Figure 10: Front view of pitch control mechanism, showing triangular rack

The pitch control design consists of a triangular rack placed in the blade hub that meshes with pinion gears attached to each blade. The triangular rack is actuated by a sled pushed by a servo motor, which is connected to the sled by a set of bearings: a thrust bearing inside of a ball bearing, so the system can displace the rotating rack without the thrust bearing rotating. The power is transferred to the motor shaft through a key that couples it with the nose cone.

Feedback Control System

One of the last aspects of our design, and one that had to be researched and designed remotely was the feedback loop control mechanism for the Arduino. The team considered using either a PI or PID controller, and decided based on the response characteristics of both systems. The control characteristics can be explained with the following equation:

$$u = K_p * e + K_i * \int_0^t e * dt + K_d * \frac{d}{dt} e \quad (3)$$

The three tuning parameters (K_p , K_i , K_d), adjust the behaviour of the controlled response, and are tuned for every application based on the desired controller characteristics. K_p controls the proportional response, which allows for a fast, smooth transition but if used by itself results in a steady state error, never reaching the desired setpoint. The K_i is the integral response, which is used in conjunction with the proportional control to eliminate this steady state error. PI controllers often result in overshoot of the desired value, resulting in continuous oscillation about the setpoint. The derivative term can mitigate this, but for some applications the oscillations are small enough that the derivative control is unnecessary.

For WiscWind's turbine, the team wanted a smooth, rapid response that can keep up with the acceleration of the wind in the competition wind tunnel. The constant oscillation of a PI control would

cost the team points for the rated power test, as the scoring is based on the ability to maintain a constant power. Because of this, the team elected to use a PID controller over a PI. The plan was to use an Arduino Uno to program and tune the PID controller, as libraries to execute PID functions are readily available. Unfortunately, due to the circumstances of this semester the team did not have the capability to fabricate a working controller prototype.

Nacelle and Yaw Control

The nacelle houses the sensitive electromechanical components of a wind turbine. Proper nacelle design allows for easy manipulation and maintenance of those components, and promotes smooth airflow around the turbine structure. The nacelle for WiseWind's turbine is shown in Figure 11.

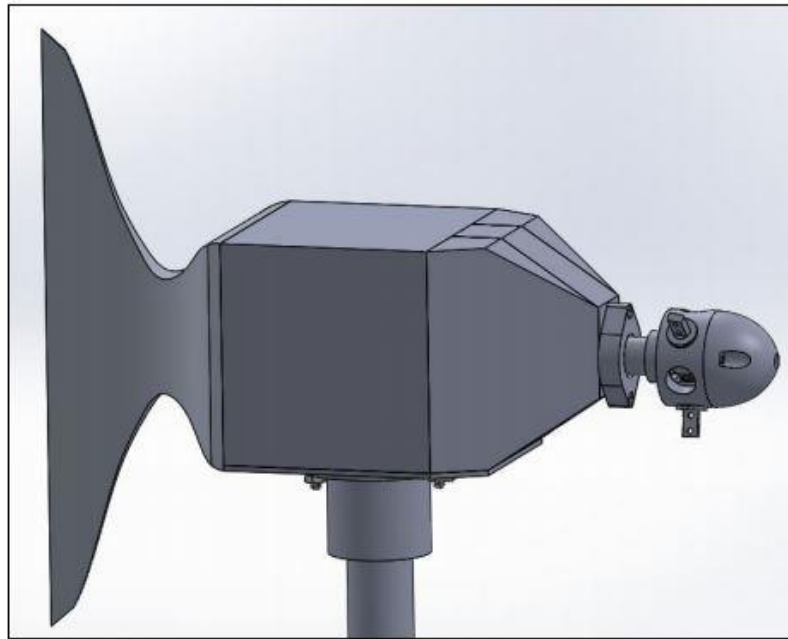


Figure 11. Nacelle and Yaw Control

The nacelle will protect sensitive interior components. The yaw control fin orients the turbine into the wind, while smooth contours in the design of these components promote better air flow.

All major electrical components are contained inside the central box section. The servo motor for the pitch control mechanism is contained within the front cone section of the nacelle, which is designed to direct wind around the turbine to reduce drag forces. There is a smooth geometric transition between the nacelle and the yaw control fin, preventing air stagnation and providing better turbine performance. The yaw control fin acts like a weathervane, with a large enough surface area and moment arm to keep the turbine blades oriented into the wind.

Both the nacelle and the yaw control fin were to be 3D-printed with PLA filament for the final assembly, but the student shops were shut down before the team was able to manufacture them. With more design time, CFD analysis and wind tunnel tests could provide insight into the aerodynamic performance of the nacelle and whether the yaw control fin could accurately orient the turbine into the wind.

Electromechanical

Electromechanical Design Objectives

The generator's physical design was created to be easily manufactured, assembled, and maintained, could be contained in one concise package for use on different turbine chassis in the future, and have extremely low friction. Electrically, the generator was designed to have zero cogging torque, create enough voltage at low speeds which would allow operation without a gearbox, have large enough gauge wires to ensure high power output, and create three-phase power that is as balanced as possible.

Mechanical Design

Design Constraints

For the 2019 competition, the size of the generator was designed to have an outer diameter of 5.5 inches and an overall length of 5.25 inches. This was used as a starting point for the design since it was deemed large enough to effectively convert mechanical to electrical energy, yet small enough to not affect the aerodynamics around the nacelle of the turbine. As we began preparing for the 2020 competition, the dimensions of the generator were changed, as we reduced our generator from three stators to just one. This cut down the assembly length to 4.25".

Stationary Components

The generator main body consists of a tube and two end caps. The end caps have shoulder features which ensure concentricity and parallelism for the bearings and rotating assembly. This allows the generator to achieve smooth and stable performance at high rotational speeds. The end caps are drawn together using three 5" long shoulder bolts. These shoulder bolts also provide mounting points for the stator inside the generator. One end cap is outfitted with a bolt hole pattern which allows the generator to be face mounted to the back of the turbine.

The stators proved to be one of the first manufacturing hurdles for the generator. The design uses a 3D-printed ring which provides structure for the stator before the coils have been cast in epoxy. The coils were placed inside the ring and connected together with a soldering iron. Finally, the stators were placed into a mold and filled with epoxy.

The stators were further improved this year. Their output leads were upgraded to a much thicker wire that was not allowed to flex at the junction of the wire to the body of the stator assembly using epoxy. This allowed the large wires to flex but not the thin enameled magnet wire. We were concerned with the strength of the thin enameled magnet wire to withstand multiple flexes, but the thicker wire is tough enough to withstand multiple bends without breaking.

Rotating Assembly

The rotating assembly consists of one main shaft and two rotors which are mounted to it. The rotors are connected to the shaft with a through pin, which provides both the rotational and translational constraints. The pin is then held in place with a collar to prevent it from sliding out while the generator is rotating.

The main problem with the 2019 team's generator design was alignment and the materials used in the alignment system. This year, the team designed and assembled a robust alignment mechanism that allowed the rotors to spin freely. The design uses two aluminum plates connected at the corners by four stainless steel threaded rods and bolts. The threaded rods cause no magnetic interference with the rotors because of their material properties, and the aluminum plates are spaced far enough from the rotors to prevent any power losses. The threaded rods allow for the precise, adjustable alignment of the stator between the rotors. A similar design was used in 2019, but issues arose because the stator was made of 3-D printed plastic which compressed when the alignment bolts were tightened. This caused the whole stator to be pinched by the rotor and resulted in unforeseen friction. Our team improved on this design by laser cutting acrylic for the outside of the stator to improve durability and reliability. The alignment system is shown in Figure 12.

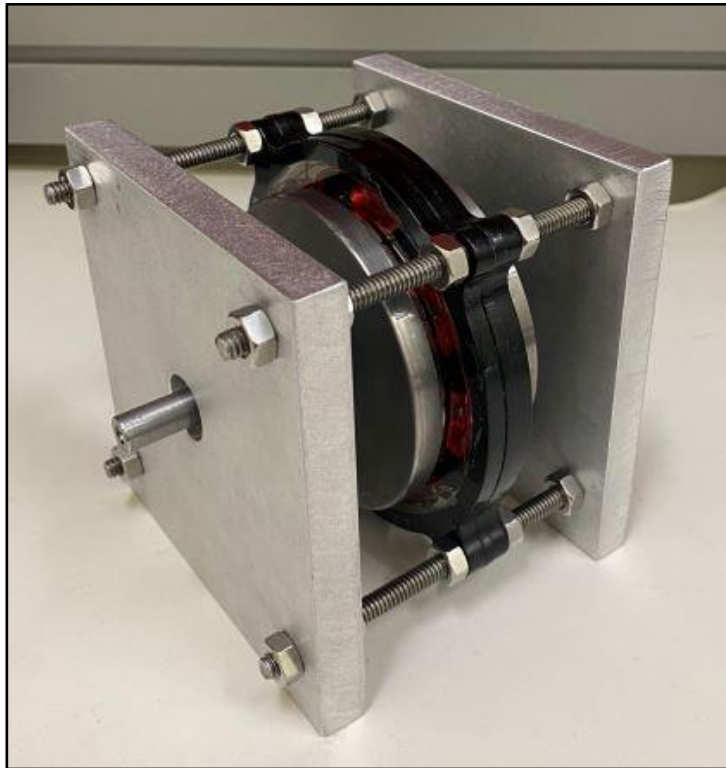


Figure 12: Generator assembly

Electrical Design

Design Constraints

The only major design constraint was the relationship between phase current and coil wire size. A wire size was chosen that provided adequate current overhead without the risk of burning out a coil or stator while remaining small enough to keep the coil fill factor high and overall generator efficiency high.

Magnets

Our team felt that the magnets used last year were a great choice again this year. They are a rounded trapezoid. This shape allows them to form a tight circle that helps reduce air gaps and overall size of the generator. The number of magnets was chosen as a baseline used last year. This number must conform to a specific ratio of coils to pole pairs so setting the number of magnets to 9 locked in the number of coils in the stator.

Coils

An important relationship to understand when designing a generator is Faraday's Law, which describes how a changing magnetic flux produces current, and therefore electric power. We used the principles of Faraday's Law to optimize the stator thickness and number of turns in each coil. The team used a Gaussmeter to model the magnetic flux density between the two stators at different distances by measuring the flux density at the magnet surface and in the center of the rotor gap. Figure 10 below shows the relationship found between magnetic flux density and position.

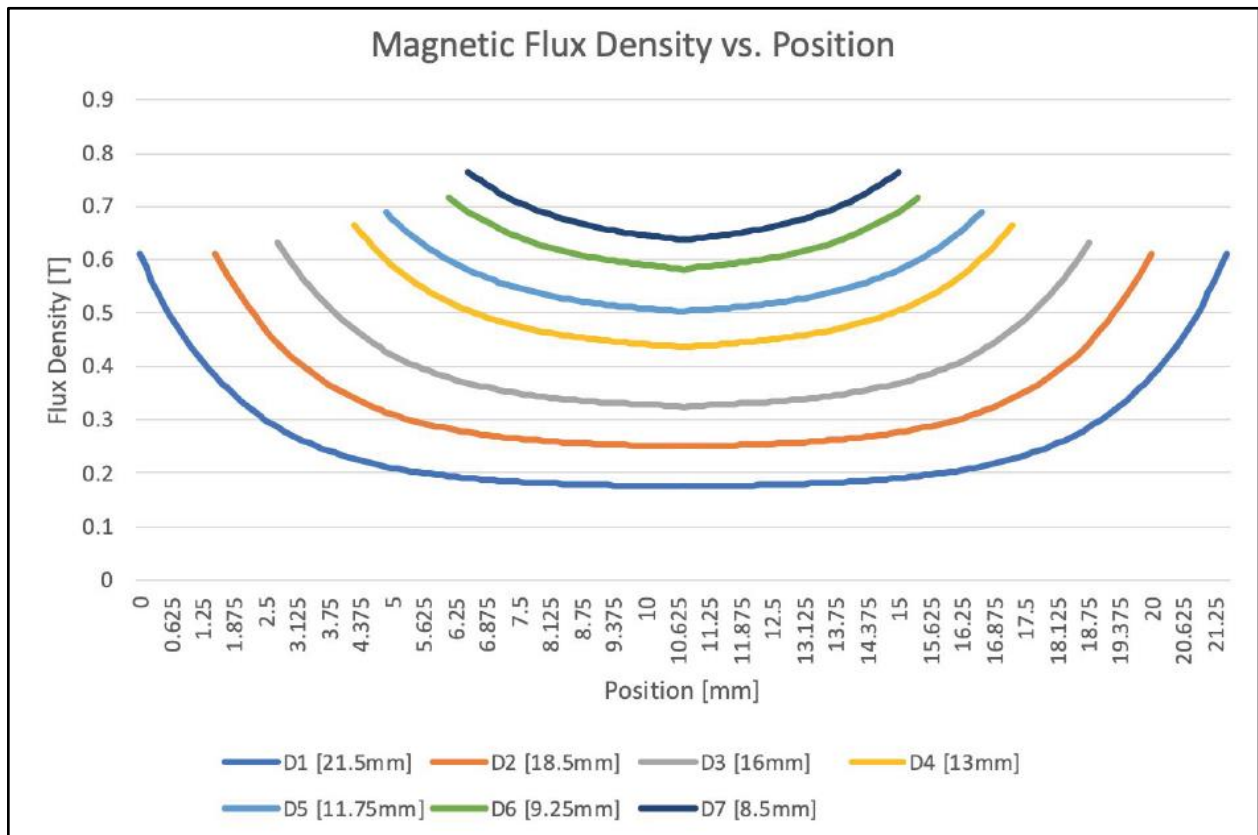


Figure 13. Magnetic flux density approximation across the rotor air gap

To allow for maximum power production, the spacing with the largest total magnetic flux, or the largest area under the curve in the figure above was chosen. Using that reasoning, a rotor spacing of 1/2" (13 mm) was chosen. After determining the stator thickness, which is the same as the rotor air gap, the optimal number of turns per coil and wire size were selected as well. A higher number of turns leads to a higher output voltage, while a larger wire diameter lowers the number of turns that can fit in the stator. The 2019 team's stator, which used 26 awg wire, was tested and produced a very high output voltage (above the 40V maximum specified by the competition) with a tiny amount of current and power. The team determined that increasing the wire size would allow more current to flow, while keeping the output voltage below the range specified by the competition. Since there is a linear relationship between the number of turns and the wire size, the number of turns is fixed at each wire size. The new stator was built with 24 AWG wire and 175 turns per coil. The new generator operated at 36V when testing the turbine at 11 m/s. The benefit of getting close to the 40V limit is a reduced cut-in wind speed, since there is a higher voltage at lower wind speeds.



Figure 14. WiscWind's stator and two rotors

Modular Design

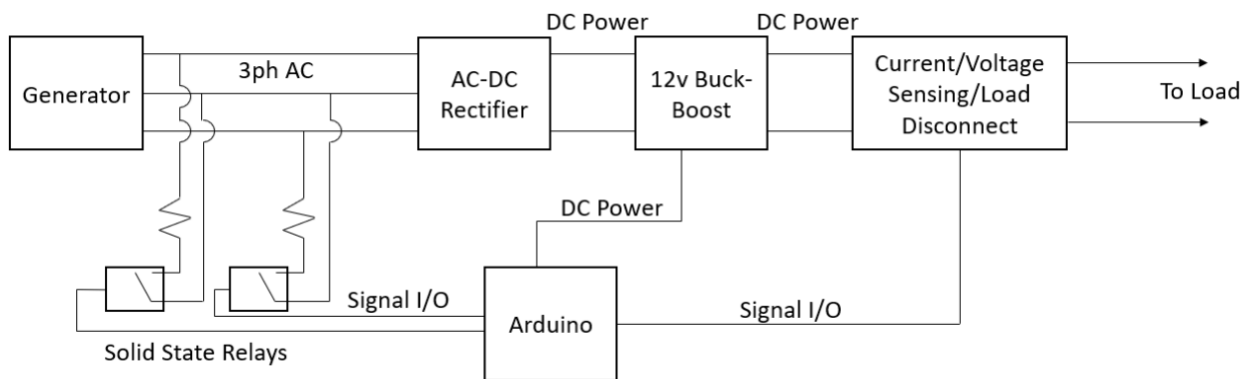


Figure 15. One-line diagram of WiscWind's modular power and safety circuitry.

Output of Generator Board

In 2019, the generator was three separate stators totalling 9 total phases. The 9 phases were then combined in series to yield 3 phase AC that could be further manipulated. This year because of the generator redesign we only have one stator producing 3 phase AC, which simplified the output from the generator.

The 2019 team decided to use a low loss active 3-phase ideal diode bridge rectifier reference design. For 2020, we are using the Linear Technology DC2465 board. On the board, there are three LT4320 IC's, which are ideal diode bridge controllers that drive six low loss N-channel MOSFETs to tell when they are on and off. The FETs are used as switching regulators, which turn on automatically without any voltage drops. This design dramatically reduces power and voltage losses. It enables the overall system to be specified to operate with a smaller, more cost-effective power supply due to the enhanced power efficiency. Low voltage applications benefit from the extra margin afforded by saving the two diode drops inherent in diode bridges. Compared to traditional approaches, the MOSFET bridge enables a rectifier design that is highly space- and power-efficient. We found the DC2465 board to be an appropriate choice

for our needs again this year and felt that using a proven solution for AC to DC conversion allowed our team to focus on other areas.

We had decided that filtering would be done by placing a capacitor across the outputs of the AC to DC converter, but because we had not finalized the electronics after that point and were also not certain on how the generator would perform, we were unable to finalize the specifications of this component.

Safety Module

The safety module of our design considers two different situations: disconnect of load, and manual or emergency shutdown. This module consists of the safety circuits and the control logics. A diagram of the final design circuit can be seen in Figure 15.

The safety circuits consist of the same two submodules of circuits and electronic components. The first submodule connects to the output of phase A and phase B, and the second submodule connects to phase B and phase C. Each submodule has a solid state relay controlled by a 5V PWM input. The PWM is generated by control logic written in Arduino. The PWM signal can vary in duty cycle from 0% to 100%, where 0% is open circuit and 100% is closed circuit. During open circuit, the low impedance/high load resistor is disconnected and the turbine operates normally. During closed circuit, the circuit applies a very large load/small resistance between the phases. This causes a very large load to be present between phase A and phase B, and between phase B and phase C. The torque of the rotor is increased greatly to the point of almost stopping, and the generator power is transferred to the resistors in the safety circuits without transferring to the load. To only slow the generator down and not necessarily stop it completely, the arduino applies a PWM signal to the relay of an intermediate duty cycle which serves to deliver a variable load to the generator. Further precision is achieved by only applying the load to two of the three phases or between all three phases. The wind turbine brakes and stops if the relay is maintained closed.

The control logic is written in Arduino that takes multiple signals as inputs and determines whether a 5V pulse signal output needs to be sent to the safety circuits to toggle the state of the relay and activate or deactivate the safety circuits. The Arduino Uno board is connected to a push button for signaling manual emergency shutdown, a current sensor for sensing load disconnect, and the relays in the safety circuits for shutting the turbine. Its power pin is also connected to the regulated output of AC/DC to make sure the control logics are always working under its rated voltage. The control logic uses a finite state machine to represent the state transitions and outputs needed under various input conditions. Initially, the state is set to 'normally operating', and the relay is opened. When the push button is pressed, the state transitions to 'button pressed', and a pulse signal is outputted to the relay to close it and shut down the turbine. Only when the button is pressed again would the state transition back to 'normally operating', and a pulse signal is outputted to the relay to open it and resume the turbine. Therefore, repeatedly pressing the push button switches the state between manual/emergency shutdown and normal operation. We also connect a current sensor in series with the load. At the state of 'normally operating', when the current sensor's current reading is 0 or close to zero, we can know that there exists an open circuit at the load and conclude that the load has been disconnected. The state transitions to 'load disconnect', and a pulse signal is outputted to the relay to close it and shut down the turbine. Only when the load is connected and the current reading becomes nonzero would the state transition back to 'normally operating', and a pulse signal is outputted to the relay to open it and resume the turbine. The finite state machine diagram is shown in Figure 16.

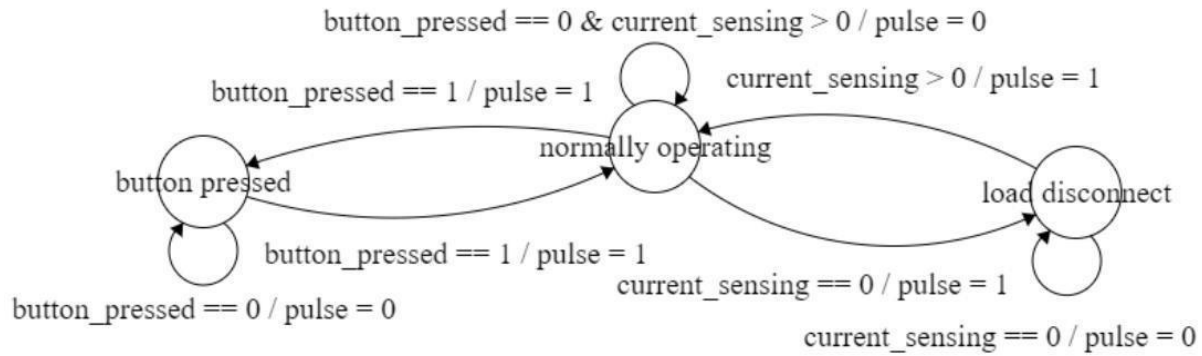


Figure 16. Finite State Machine of Safety board

Preceding the Arduino in the circuit is the DROK DC/DC Automatic Buck Boost Converter. This Buck Boost converter is used to supply a constant voltage to the Arduino in order to make sure it is always powered on and thus able to divert power to the safety system if required. It is rated for input voltages varying from 5V to 32V and is set to constantly output 12V for the Arduino. Table 1 below includes our results from voltage testing.

Table 1: DROK Voltage Regulation Testing Results

Input Voltage	Output Voltage
5.34 V	12.061 V
9.21 V	12.063 V
12.60 V	12.064 V
15.47 V	12.059 V
18.78 V	12.059 V

Testing and Results

Testing of Emergency Braking

The team was unfortunately unable to complete nearly as much testing as we had hoped. Testing was limited to the generative braking system. The generative braking was engaged by using a prototype of the emergency braking system. We began by spinning up the generator while connected to a 60 ohm load. We then initiated emergency braking, which caused the Arduino to PWM the Solid State Relay. There was one relay connected as described above in the Safety section to a 1 ohm load. Competition rules dictate that the turbine speed must be reduced to less than ten percent of rated value. Figure 17 below shows the ability for the generative braking to reduce the wind turbine speed as the competition requires. The turbine was operating at a wind speed of 11 m/s and at 1460 RPM when braking was engaged.

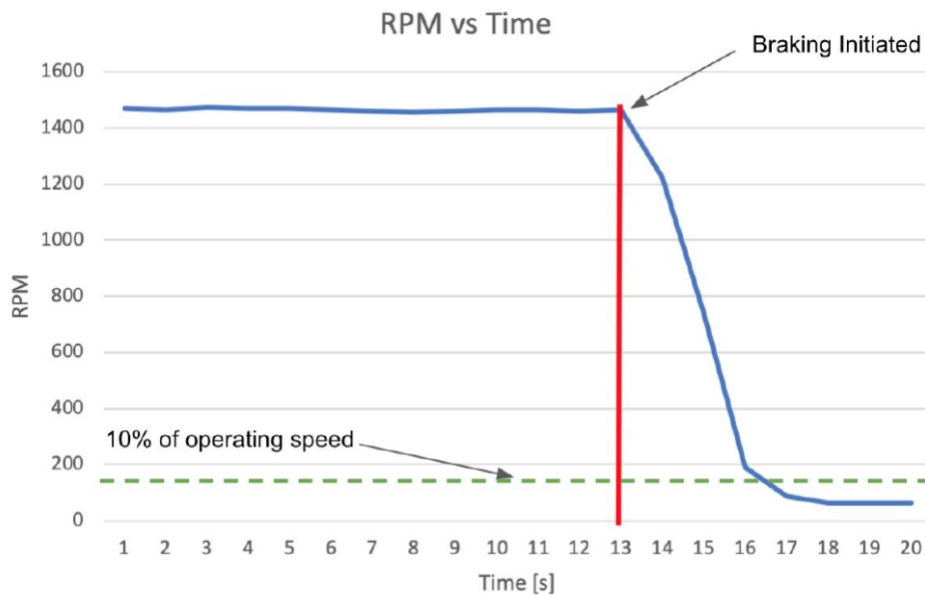


Figure 17. Generative braking wind tunnel test.

Conclusion

Although the 2020 WiscWind team did not complete the prototype assembly and manufacturing, the team gained a lot of design insights that will set the team up for future success. Successes include iterative blade design and testing, custom generator fabrication, and an emergency braking system prototype. Unfinished tasks include implementing the planned pitch control system, fabricating a final set of competition blades, designing and fabricating the hub cover and the yaw control system, and implementing the final power and control circuitry. However, next year's team may draw from the design plans laid out in this report to set themselves up to perform well in the 2021 competition and hopefully bring to life many elements of the turbine that this year's team envisioned.

References

- [1] “Typical wind turbine power curve : the turbine begins to operate at the... | Download Scientific Diagram.” https://www.researchgate.net/figure/Typical-wind-turbine-power-curve-the-turbine-begins-tooperate-at-the-cut-in-speed-v-c_fig3_320686586 (accessed Apr. 30, 2020).
- [2] “Betz limit - Energy Education.” https://energyeducation.ca/encyclopedia/Betz_limit (accessed Apr. 30, 2020).
- [3] S. translations based on Olivier Cleynen work and Nubifer, English: Definition of the chord length on an airfoil. 2018.
- [4] “Air - Altitude, Density and Specific Volume.” https://www.engineeringtoolbox.com/air-altitude-density-volume-d_195.html (accessed Apr. 30, 2020).
- [5] R. Gasch and J. Twele, “Blade geometry according to Betz and Schmitz,” in *Wind Power Plants: Fundamentals, Design, Construction and Operation*, R. Gasch and J. Twele, Eds. Berlin, Heidelberg: Springer, 2012, pp. 168–207.
- [6] “XFOIL.” [Online]. Available: <http://web.mit.edu/drela/Public/web/xfoil/>. [Accessed: 22-Sep2019].
- [7] “QBlade.” [Online]. Available: <http://www.q-blade.org/>. [Accessed: 22-Sep2019].